CHEMISTRY
A EUROPEAN JOURNAL

DOI: 10.1002/chem.201101551

How Does Cu^{II} Convert into Cu^{I}? An Unexpected Ring-Mediated Single-Electron Reduction

Davide Barreca,[b] Ettore Fois,[a] Alberto Gasparotto,[c] Roberta Seraglia,[b] Eugenio Tondello,[c] and Gloria Tabacchi*[a]

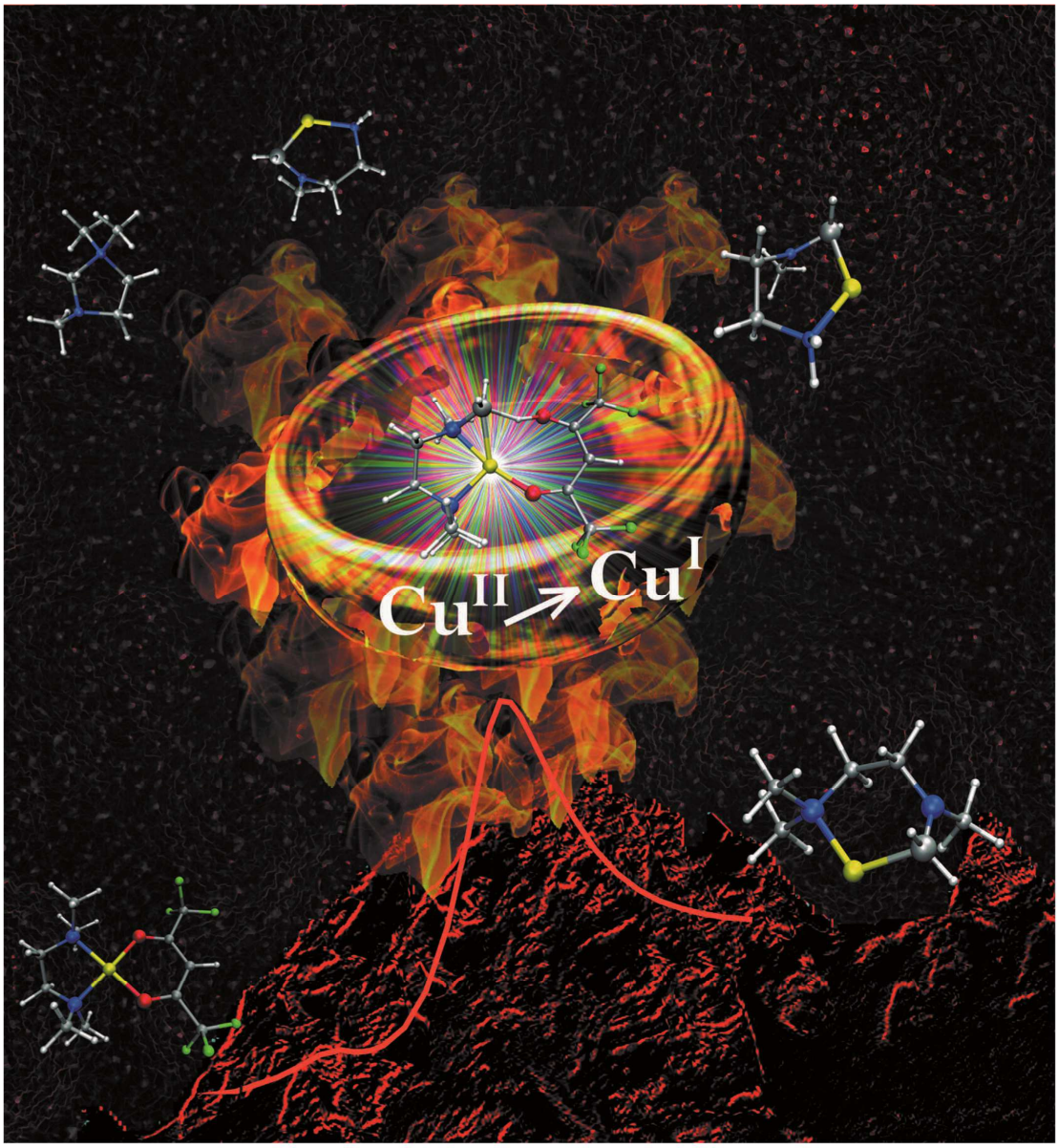

WILEY ONLINE LIBRARY

© 2011 Wiley-VCH Verlag GmbH & Co. KGaA, Weinheim

To be cited as: Chem. Eur. J., 17: 10864–10870. doi: 10.1002/chem.201101551
Version of record: http://dx.doi.org/10.1002/chem.201101551

How does Cu^{II} convert into Cu^{I}?

An unexpected ring-mediated single-electron reduction

Davide Barreca,[b] Ettore Fois,[a] Alberto Gasparotto,[c]

Roberta Seraglia,[b] Eugenio Tondello,[c] and Gloria Tabacchi*[a]

[a] Prof. E. Fois, Dr. G. Tabacchi
Department of Chemical and Environmental Sciences, University of Insubria and INSTM
Via Lucini 3, 22100 Como, Italy
Fax: (+)39 031 2386630
e-mail: gloria@fis.unico.it

[b] Dr. D. Barreca, Dr. R. Seraglia
Department of Chemistry, CNR-ISTM and INSTM and Padova University
35131 Padova, Italy.

[c] Dr. A. Gasparotto, Prof. E. Tondello
Department of Chemistry, INSTM and Padova University
35131 Padova, Italy.

To be cited as: Chem. Eur. J., 17: 10864–10870. doi: 10.1002/chem.201101551
Version of record: http://dx.doi.org/10.1002/chem.201101551

Abstract: Currently up in the agenda of sustainable technologies, Cu_xO (x = 1,2) nanomaterials with tailored composition and properties may be fabricated from molecular sources through bottom-up processes involving unexpected changes in the metal oxidation state that open intriguing challenges on the copper redox chemistry. How copper(II) sources may lead to copper(I) species in spite of the absence of any explicit reducing agent, and even in the presence of oxygen, is one of such questions – to date unanswered. In this work, we have studied copper "reduction without reductants" within one molecule and revealed that the actual reducing agent is abstracted atomic hydrogen. Investigating the fragmentation of a copper(II) precursor for copper oxides nanostructures by combined Electrospray Ionization Mass Spectrometry with multiple collisional experiments (ESI/MS^n) and theoretical calculations, we highlighted a copper-promoted C-H bond activation, leading to reduction of the metal center and formation of a Cu^I-C-NCCN six-membered ring. Such a novel ring system is the structural motif for a new family of cyclic copper(I) adducts which show a bonding scheme, herein reported for the first time, that may shed unprecedented light on copper chemistry. Beyond its relevance for the preparation of copper oxide nanostructures, the "hydrogen abstraction-proton delivery-electron gain" mechanism of copper(II) reduction here disclosed appears to be a general property of copper and might help to understand its redox reactivity.

To be cited as: Chem. Eur. J., 17: 10864–10870. doi: 10.1002/chem.201101551
Version of record: http://dx.doi.org/10.1002/chem.201101551

Introduction

Molecular-level understanding of complex chemical events is the key for optimally designing and controlling processes of great technological relevance, such as molecule-to-nanosystem conversion approaches.[1-5] Novel and unexpected reactivity at the gas-solid or liquid-solid interfaces may indeed enable the development of materials with unique structure and properties for new applications. Among the flourishing of advanced systems obtained by molecular routes, nanostructures based on copper(I,II) oxides (Cu_xO, with x = 1,2) deserve major attention for their broad uses in the field of sustainable development.[6-10] Copper(II) oxide is indeed an ideal candidate for the fabrication of optical switches, photoconductive devices, sensors and Li-ion batteries due to its excellent electrical and optical properties.[6] Solar radiation may also be converted into storable chemical energy by CuO nanomaterials, making thus feasible hydrogen generation by photo-assisted routes.[10] Ecocompatibility is a distinctive feature even for Cu_2O, an excellent catalyst for the photodegradation of organic pollutants under visible light, whereas copper and copper oxide nanoparticles embedded in silica matrices further extend the technological applications of such materials.[11] In the design of nanoarchitectures for the production of advanced devices, the ability to develop Cu-O systems with controlled composition and nano-organization is crucial, but the lack of information on the underlying chemical processes still hampers a systematic and knowledge-based design of fabrication procedures.[12,13] Very little is known about the microscopic routes turning molecules into materials, especially when redox changes occur and unexpected products are obtained. For example, the formation of copper(I) species from copper(II) sources in the absence of any explicit reducing agent - observed in many experiments and, in some cases, even under oxidizing conditions – has been an intriguing chemical enigma since the early ages of bottom-up technologies.[11,13,14,15] In spite of many progresses, the evolution of the copper oxidation state from the precursor to the material is still matter of speculation and the strange case of copper reduction 'without reductants', a missing piece in the basic chemistry of this element, still remains an open and intriguing challenge. The observation of this surprising phenomenon, detected for several fabrication approaches under different conditions, suggests that its origin should lie in the copper molecular sources themselves. On this basis, we challenged the 'reduction without reductants' enigma at the single molecule level and report herein the first observation of a $Cu^{II} \rightarrow Cu^{I}$ reduction within one molecule and without any external reducing agent.

Our case study is the *β*-diketonate diamine complex of copper(II) with hfa (1,1,1,5,5,5-hexafluoro-2,4-pentanedionate) and TMEDA (*N*,*N*,*N*',*N*'-tetramethylethylenediamine) [$Cu(hfa)_2$(TMEDA)], a successful example of copper molecular precursor with favourable properties for the growth of Cu_xO (x = 1,2) nanostructures.[13,16] Here, the copper(II) center is octahedrally coordinated by four oxygen and two nitrogen atoms (see Figure 1). Integrated experimental and computational analyses have recently enabled us to clarify the bonding structure of the above compound[17] and to grasp some appealing aspects of its activation at "hot" surfaces, a relevant issue for Chemical Vapor Deposition (CVD) processes where the surface of the growing material can further enhance the precursor reactivity.[18] In spite of such advancements, its actual decomposition pathway on a molecular scale remains so far unknown.

By a powerful combination of ESI/MS^n experiments and theoretical investigations, this work establishes the gas phase fragmentation mechanism of the precursor complex, provides key elements to tackle its conversion to copper oxides nanostructures, and reveals how copper reduction without reductants occurs. We will show that the actual reducing agent is hydrogen, which is extracted, as an atom, from a ligand and collected, as a proton, by another ligand

To be cited as: Chem. Eur. J., 17: 10864–10870. doi: 10.1002/chem.201101551
Version of record: http://dx.doi.org/10.1002/chem.201101551

within the same molecule, so that no external reductant is needed. In the specific, copper(II) gains an electron by assisting a simultaneous C-H bond cleavage - interligand proton transfer, leading to a new copper(I)/radical ligand complex with a Cu^{I}-C-NCCN six-membered ring. Overall, the results reported in the following disclose an unprecedented example of C-H bond activation, uncover a novel type of copper-carbon bonding scheme and reveal that copper(II) can promote a $H^{\bullet} \rightarrow H^{+}$ conversion *via* a simple "hydrogen abstraction-proton delivery-electron gain" process. This copper(II)-copper(I) reduction channel features itself as a general property of copper, which might emerge in a broad variety of chemical contexts, and, in principle, whenever copper(II) comes in contact with both a hydrogen 'source' and a proton 'drain'.

Results and Discussion

As a starting point, we discuss the calculated M06/D95+*[19-21] minimum energy structure of the $[Cu(hfa)(TMEDA)]^{+}$ ion, detected as the most abundant species at *m/z* (mass-to-charge ratio) 386.04842 (theoretical value: 386.04847, elemental formula $C_{11}H_{17}F_6N_2O_2Cu$) in the high resolution positive mode ESI/MS spectrum of $[Cu(hfa)_2(TMEDA)]$ methanolic solutions.[17] In $[Cu(hfa)(TMEDA)]^{+}$, copper is coordinated to two *β*-diketonate oxygens and two diamine nitrogens with distances of 1.913 and 2.016 Å respectively, in a C_2-symmetric regular square planar geometry (Figure 2). Electronic structure and spin density analyses, and inspection of the molecular orbitals, show that one of the metal β-d states is empty, confirming that copper is in the II redox state (Figures 3 and 4). The two ligands are more tightly bound to the Cu center than in the parent neutral complex, as testified by the strengthening of metal-ligand interactions and the concurrent shortening of coordination distances (see Table S1). Collisional experiments indicate that the decomposition pathway of this species involves the loss of a proton mass from TMEDA, leading to a dehydrogenated diamine species TMEDA(-H), the net transfer of a proton to hfa and the release of a neutral Hhfa *β*-diketone. As evidenced in Figure 1a, the ESI/MS^2 mass spectrum of the $[Cu(hfa)(TMEDA)]^{+}$ ion shows an abundant peak at *m/z* = 178.05250, corresponding to a species where copper is coordinated by TMEDA(-H).

This result is confirmed by the ESI/MS^3 mass spectrum of this ion (Figure 1b), which shows peaks directly correlated with the TMEDA ligand. In fact, the ions at *m/z* 163.02911 and 134.00253 correspond to the loss of a methyl and a $(CH_3)_2N$ radicals, respectively, while the ion at *m/z* 115.12287 can be assigned to $[C_6H_{15}N_2]^{+}$ ionic species.

Since the $[Cu(hfa)(TMEDA)]^{+}$ optimized geometry provided no hints on the interpretation of these data, we tried to shed light by modeling the finite temperature behavior of the ion. Interestingly, the exploratory first principles molecular dynamics (FPMD) simulations[22] at T = 473 K evidenced fluctuations from the square planar geometry, typical of the minimum energy structure, to a twisted tetrahedral arrangement with the two ligands roughly perpendicular to each other. These results suggest that such a distortion might promote the observed fragmentation of $[Cu(hfa)(TMEDA)]^{+}$ and can be accessed by providing sufficient energy to this species. To gain an insight into the fragmentation mechanism, we performed on $[Cu(hfa)(TMEDA)]^{+}$ FPMD simulations combined with blue-moon ensemble statistical sampling, a technique enabling to investigate reactive events through the choice of a suitable constraint (reaction coordinate).[23] As a matter of fact, the loss (gain) of a proton mass of the diamine (*β*-diketonate) requires one C-H and one O-H bond to be broken and formed, respectively. To minimize possible biases in the reaction path exploration, we chose as reaction coordinate the difference of the distances of a diamine methyl proton, H*, from its carbon atom C* and from the farthest diketonate oxygen atom O* (see Figure 2 and supporting movie).

Along the calculated pathway, we initially observed the ion switching from a square planar to a twisted tetrahedral geometry, as in the exploratory unconstrained simulation. Subsequently, after a 180° out-of-plane rotation of the

To be cited as: Chem. Eur. J., 17: 10864–10870. doi: 10.1002/chem.201101551
Version of record: http://dx.doi.org/10.1002/chem.201101551

diketonate, the C*-H* bond gradually approaches the oxygen atom O*, while becoming increasingly elongated and closer to the metal center. Afterwards, the activated C-H moiety displaces the diketonate oxygen away from its coordination position, leading to a structure where the aliphatic proton is on the fly between the two ligands, and the diamine acts as a polydentate ligand towards Cu. Full transfer of the proton to the diketonate oxygen leads to a *β*-diketone enol and to an *α*-dehydrogenated diamine, the latter closing a six-membered ring with its C-terminal coordinating the copper center. In order to confirm these observations, we accurately located transition and final states by hybrid Density Functional Theory (DFT) optimizations (Figure 2) and investigated their electronic structures. The proof of copper reduction is the full occupancy of its d-shell at the end of the process (Figure 3), whereas the spin density distribution in the transition state, showing the formation of a TMEDA(-H)$^{\bullet}$ radical moiety, reveals that the C-H bond cleavage is homolytic (Figure 4b). As a result, copper is finally in the (I) oxidation state, bound to the neutral *β*-diketone enol and to the N,C bidentate radical ligand TMEDA(-H)$^{\bullet}$. Since all observed chemical events - coordination sphere rearrangement by rotation, C-H bond activation, interligand proton transfer, copper reduction and ring formation - occur within the same ionic species, and the *α*-dehydrogenated diamine attacks Cu in the form of a radical, we nickname this reaction single-molecule single-electron cyclocupration. Not surprisingly, the barrier amounts to 59.8 kcal/mol and the process is endoergonic, with the optimized (Hhfa)[Cu^{I}(TMEDA(-H))]$^{+\bullet}$ 'product' 34.5 kcal/mol higher in energy than the optimized [Cu^{II}(hfa)(TMEDA)]$^{+}$ 'reactant'.

The metal role in the C-H activation process is evident from both the transition state geometry and electronic structure, illustrated in Figures 2-4. The transition state, with Cu-C and Cu-H distances of 2.125 and 2.001 Å respectively, exhibits a distorted square planar geometry reminiscent of the initial [Cu(hfa)(TMEDA)]$^{+}$ structure, but with the cleaving C-H bond formally replacing one of the diketonate oxygens in the copper coordination sphere. Here, the C-H bond is activated, as indicated by the C*-H* and O*-H* distances (1.459 and 1.227 Å, respectively) and by the structural perturbations of the diamine and *β*-diketonate ligands. The transition state electronic structure (Figure 2, top panels) and spin density (Figure 4b) reveal the incipient formation of an O-H bond and the appearance of an *α*-amino radical, and clearly illustrate the active participation of the copper d states in this process. Meanwhile, the metal d_{x2-y2} orbital, empty in the initial state, is being filled, as deduced from the partial Cu-d character of the HOMO (Figure 3, center) and from the spin density decrease on copper (Figure 4b). Hence, the metal center activates the *α*-amino C-H bond by smoothly shuttling the proton on the diketonate oxygen, while gaining one electron for its role of mediator. The whole process ends up with copper in the d^{10} configuration, coordinated to the neutral Hhfa ligand and forming with TMEDA(-H)$^{\bullet}$ a six-membered ring adduct with a chairlike conformation (see Figures 2-3, lower left panels). The copper(I) "chair" shows spin density predominantly localized on the C*N* moiety, representing thus the first known example of a cyclic copper(I) complex with a radical ligand (Figure 4c). To check its stability as isolated species, we removed the *β*-diketone enol ligand and optimized the resulting geometry. We observed that the six-membered ring is maintained and both Cu-N and Cu-C* bonds are shortened. As a result, the chair structure enlarges along the N-C* axis leading to the [Cu(TMEDA(-H))]$^{+\bullet}$ 'armchair' represented in Figures 4d and 5.

There are various reasons to believe that this species corresponds to the ion detected at *m/z* = 178.05250 in the ESI/MS^2 spectrum of [Cu(hfa)(TMEDA)]$^{+}$ ion (*m/z* = 386.04842) (Figure 1). First of all, the N,C bidentate [Cu(TMEDA(-H))]$^{+\bullet}$ is energetically favored in comparison to other possible candidates, for instance, by 28.8 kcal/mol with respect to the N-monodentate adduct, as corroborated by extensive higher level of theory tests (MP2 and CCSD(T), see Supporting Information). Moreover, the minimum energy geometries calculated for the MS^3 fragment ions evidence that the six-membered ring structure is compatible with the experimental fragmentation pattern of the ion at *m/z* = 178.05250 and is the structural leitmotif of the most abundant Cu-containing MS^3 fragment ions (see Figure 1). Finally, the copper(I)

To be cited as: Chem. Eur. J., 17: 10864–10870. doi: 10.1002/chem.201101551
Version of record: http://dx.doi.org/10.1002/chem.201101551

binding energy with the diamine radical, 118.5 kcal/mol, suggests a remarkable stability of this peculiar cyclic system and points out to strong Cu-N and Cu-C* bonds. Indeed, electronic structure analyses prove that these bonds are partially covalent, as indicated by the significant contribution of the copper(I) d states to the molecular orbitals bonding with respect to Cu-N and Cu-C* (Figure 5c). We also observed that the α-HOMO has (C*N*)-π*character and that the C*-N* bond length, 1.387 Å, is shorter compared to the other C-N distances, evidencing thus a partial C*-N* double bond character. Together with these observations, the delocalization of the spin density over the Cu-C*-N* moiety reveals a three electrons-three centered π-type Cu-C-N bond. Remarkably, even non covalent interactions play a key role in stabilizing the cyclic copper(I) complex, as demonstrated by Natural Bond Orbital[24] analyses (Table S6): donation from the ligand (C*N*)-π bonding orbital to the vacant Cu 4s state, and backdonation from the occupied Cu d orbitals to the vacant ligand (C*N*)-π* antibonding orbital further favor the six-membered ring structure of $[Cu(TMEDA(-H))]^{+\bullet}$ over the N-monodentate arrangement, where these interactions are absent. This complex and fascinating bonding scheme, here highlighted for the first time, could lie at the origin of a new class of ring-shaped Cu^{I}-radical ligand adducts.

Conclusion

The novel features of the copper redox properties here unraveled underline the potentialities of the integrated ESI/MS^n - computational approach in disclosing important aspects of molecular reactivity. $Cu^{II} \rightarrow Cu^{I}$ reduction within a single molecular species was achieved in the MS-MS fragmentation of a copper(II) complex, where a copper-promoted C-H bond activation led to a cyclic Cu^{I}-N,C bidentate radical ligand adduct, characterized by a six-membered ring structure with an armchair-like conformation. With the assistance of Cu, a hydrogen atom was abstracted from a C-H bond of the diamine TMEDA ligand and transferred as a proton to the electron-rich and negatively charged *β*-diketonate hfa. The proton-accepting ligand was subsequently eliminated as a neutral *β*-diketone enol in the mass fragmentation process and the novel six-membered ring copper(I) complex $[Cu(TMEDA(-H))]^{+\bullet}$ was detected and characterized. Our observations, unraveling unexpected features of copper chemistry, are corroborated and rationalized by high-level calculations on the reaction transition and final state. Hybrid DFT results demonstrate that copper(II) gains one electron and is reduced to copper(I) by mediating a hydrogen abstraction - interligand proton transfer process in $[Cu(hfa)(TMEDA)]^{+}$. The transition state electronic structure indicates a homolytic C-H bond cleavage, which converts TMEDA in a *α*-dehydrogenated radical ligand, and shows that the O-H bond formation is accompanied by a simultaneous electron transfer into the vacant Cu d_{x2-y2} state. On this basis, the novel reaction here reported can be regarded as an intramolecular single-electron cyclocupration. The calculated endotermicity and high energy barrier, compatible with the experimental conditions here adopted and in line with calculations on other collision-induced reactions,[25] are due to hydrogen atom abstraction from the diamine. In $[Cu(hfa)(TMEDA)]^{+}$, both ligands are bidentately-coordinated to copper in a square planar geometry and therefore subjected to severe sterical restrictions, which unfavor the entrance of the TMEDA methyl C-H bond in Cu coordination sphere. We hypothesize that the presently observed single-electron copper reduction mechanism may take place with a lower barrier in other copper(II) species where the ligand geometry and spatial arrangement could enable an easier approach of the cleaving C-H bond to the copper center. Indeed, copper reduction *via* the hydrogen abstraction – proton transfer – electron gain scheme can in principle take place within each molecular copper(II) complex containing both hydrogen-bearing ligands and Broensted basic ligands, and in all cases where hydrogen donor and proton accepting moieties have a simultaneous access to copper. In these conditions, copper(II) may trigger homolytic cleavage of strong X-H bonds, and convert a hydrogen atom into a bare proton by

To be cited as: Chem. Eur. J., 17: 10864–10870. doi: 10.1002/chem.201101551
Version of record: http://dx.doi.org/10.1002/chem.201101551

abstracting its electron. Our results suggest that abstracted atomic hydrogen may be the actual copper(II) reducing agent in many other processes occurring at high energies or high temperatures, and pave the way to the understanding of copper(II) molecular reactivity under non-standard conditions, *e.g.* such as those of CVD processes.

As regards the molecular precursor used for Cu_xO (x = 1,2) nanostructure production, our results show that the $[Cu(hfa)_2(TMEDA)]$ precursor is intrinsically prone to undergo a $Cu^{II} \rightarrow Cu^{I}$ reduction at the expense of H atom abstraction, oxidation, and ligand release. As we expect this feature to be common to copper(II) molecular species with H-bearing/proton accepting ligands, this study provides a rationale for the observed and unexpected Cu reduction taking place in bottom-up syntheses of copper oxides,[13-15] where very high temperatures (> 700 K) are needed to promote the obtainment of copper(II) oxides over copper(I) species under oxidizing conditions.[13] Nevertheless, further investigation on the actual molecule-to-nanostructure production process is required and work is actually in progress in our laboratories.

Experimental and Computational Section

The $[Cu(hfa)_2(TMEDA)]$ complex was synthesized by following a previous procedure.[17] All positive ions ESI/MS and ESI/MS^n measurements were performed on an LTQ Orbitrap (ThermoFisher Scientific, Bremen Germany), using a resolution power of 60000 at *m/z* 400 (FWHM). The entrance capillary temperature and voltage were set at 280°C and 5 kV, respectively. 10^{-6} M solution of the $[Cu(hfa)_2(TMEDA)]$ complex in methanol were introduced in the ESI source by a syringe pump at a flow rate of 8 μL/min. MS^n experiments were performed in the linear ion trap, utilizing Orbitrap as high resolution mass analizer for the fragments. An isolation width of 1 amu was used and the precursors were fragmented with a normalized collision energy of 30 - 25%.

Hybrid Density Functional Theory (DFT) calculations on the $[Cu(hfa)_2(TMEDA)]$ complex, on the $[Cu(hfa)(TMEDA)]^+$ and $[Cu(TMEDA\text{-}(H))]^{+\bullet}$ species, and on the fragment ions in the MS^3 spectrum, with spin multiplicity 2, were performed with the Gaussian 09 (G09) code.[21] Optimized geometries and vibrational frequencies were calculated with the unrestricted M06 functional[19] in combination with an ECP10-MDF pseudopotential,[26] the aug-cc-pVDZ-PP basis for Cu,[27] and full double zeta plus diffuse and polarization functions (D95+*) basis set[20] for the ligand atoms. All calculated minima had positive frequencies; the transition state was characterized by a single imaginary frequency. Electronic structure analyses on the M06 optimized geometries were performed with the aug-cc-pVTZ basis set for the ligand atoms. Energy differences and Basis Set Superposition Error corrected binding energies were calculated with M06/aug-cc-pVTZ wavefunctions on the M06/D95+* optimized geometries. M06 results were validated by performing on $[Cu(TMEDA\text{-}(H))]^{+\bullet}$ test calculations at the MP2 and CCSD(T) levels of theory. The results, reported in the supporting information, confirmed the reliability of the adopted hybrid DFT scheme, in line with current literature studies.[28] High temperature effects on the $[Cu(hfa)(TMEDA)]^+$ and $[Cu(TMEDA\text{-}(H))]^{+\bullet}$ ionic species, typical of ESI/MS^n conditions, were investigated by first principles molecular dynamics (FPMD).[22] The exploratory reaction pathway was obtained by combining FPMD with the bluemoon ensemble technique.[23] The PBE functional, plane wave basis sets and ultra-soft pseudopotentials[29] were used. An isolated cubic box of 1.8 nm of size and plane wave cut-off values of 30 and 240 Ry for orbital expansion and electronic density representation, respectively, were adopted. A time step of 0.121 fs and an inertia parameter of 500 atomic units (au) for the electronic coefficients were used for the trajectory integration.[22] Calculations were performed at the Centro di Calcolo Scientifico of Insubria University.

To be cited as: Chem. Eur. J., 17: 10864–10870. doi: 10.1002/chem.201101551
Version of record: http://dx.doi.org/10.1002/chem.201101551

Acknowledgements

The research leading to these results has received funding from Padova University PRAT 2010 project "Innovative multi-functional nanosystems for hydrogen production and sensing". Dr. Mario Oriani (Centro di Calcolo Scientifico of Insubria University) is gratefully acknowledged for technical support.

References

[1] P. Alivisatos, P. F. Barbara, A. W. Castelman, J. Chang, D. A. Dixon, M. L. Klein, G. L. McLendon, J. S. Miller, M. A. Ratner, P. J Rossky, S. I. Stupp, M. E. Thompson, *Adv. Mater.* **1998**, *10*, 1297-1336.

[2] G. Condorelli, G. Malandrino, I. Fragalà, *Coord. Chem. Rev.* **2007**, *251*, 1931-1950.

[3] L. Armelao, D. Barreca, G. Bottaro, A. Gasparotto, S. Gross, C. Maragno, E. Tondello, *Coord. Chem. Rev.* **2006**, *250*, 1294-1314.

[4] S. Aldridge, *Dalton Trans.* **2008**, *26*, 3377-3377.

[5] R. Ciriminna, M. Sciortino, G. Alonzo, A. de Schrijver, M. Pagliaro, *Chem. Rev.* **2011**, *111*, 765-789.

[6] X. P. Gao, J. L. Bao, G. L. Pan, H. Y. Zhu, P. X. Huang, F. Wu, D. Y. Song, *J. Phys. Chem. B* **2004**, *108*, 5547-5551.

[7] G. Papadimitropoulos, N.Vourdas, V. E. Vamvakas, D. Davazoglou, *Thin Solid Films* **2006**, *515*, 2428-2432.

[8] J. L. Deschanvres, C. Jimenez, L. Rapenne, N. McSporran, B. Servet, O. Durand, M. Modreau, *Thin Solid Films* **2008**, *516*, 1461-1463.

[9] C. J. Engel, T. A. Polson, J. R. Spado, J. A. Bell, A. Fillinger, *J. Electrochem. Soc.* **2008**, *155*, F37-F42.

[10] D. Barreca, P. Fornasiero, A. Gasparotto, V. Gombac, C. Maccato, T. Montini, E. Tondello, *ChemSusChem* **2009**, *2*, 230-233.

[11] L. Armelao, D. Barreca, G. Bottaro, G. Mattei, C. Sada, E. Tondello, *Chem. Mater.* **2005**, *17*, 1450-1456.

[12] A. Radi, D. Pradhan, Y. Sohn, K. T. Leung, *ACS Nano* **2010**, *4*, 1553-1560.

[13] D. Barreca, A. Gasparotto, C. Maccato, E. Tondello, O. I. Lebedev, G. van Tendeloo, *Cryst. Growth Des.* **2009**, *9*, 2470-2480.

[14] J. Medina-Valterra, J. Ramirez-Ortiz, V. M. Arrojo-Rojas, P. Bosh, J. A. delost Reyes, *Thin Solid Films* **2002**, *405*, 23-28.

[15] J. Pinkas, J. C. Huffman, D. V. Baxter, M. H. Chisholm, K. G. Caulton, *Chem. Mater.* **1995**, *7*, 1589-1596.

[16] S. Delgado, A. Muñoz, M. E. Medina, C. J. Pastor, *Inorg. Chim. Acta* **2006**, *359*, 109-117.

[17] G. Bandoli, D. Barreca, A. Gasparotto, R. Seraglia, E. Tondello, A. Devi, R. A. Fischer, M. Winter, E. Fois, A. Gamba, G. Tabacchi, *Phys. Chem. Chem. Phys.* **2009**, *11*, 5998-6007.

[18] E. Fois, G. Tabacchi, D. Barreca, A. Gasparotto, E. Tondello, *Angew. Chem.* **2010**, *122*, 1988–1992; *Angew. Chem. Int. Ed.* **2010**, 49, 1944-1948.

[19] Y. Zhao, D. G. Truhlar, *Theor. Chem. Acc.* **2008**, *120*, 215-241.

[20] T. H. Dunning Jr., P. J. Hay, in: *Modern Theoretical Chemistry, Vol. 3* (Eds: H. F. Schaefer, III), Plenum: New York, **1976**, pp.1-28.

To be cited as: Chem. Eur. J., 17: 10864–10870. doi: 10.1002/chem.201101551
Version of record: http://dx.doi.org/10.1002/chem.201101551

[21] Gaussian 09, Revision D.02; M. J. Frisch *et.al.*, Gaussian, Inc., Pittsburgh PA, **2010**.

[22] R. Car, M. Parrinello, *Phys. Rev. Lett.* **1985**, *55*, 2471-2474; CPMD Program, www.cpmd.org.

[23] E. A. Carter, G. Ciccotti, J. T. Hynes, R. Kapral, *Chem. Phys. Lett.* **1989**, *156*, 472-475.

[24] A. E. Reed, L. A. Curtiss, F. Weinhold, *Chem. Rev.* **1988**, *88*, 899-916; NBO Version 3.1, E. D. Glendening, A. E. Reed, J. E. Carpenter, F. Weinhold, Theoretical Chemistry Institute, University of Wisconsin, Madison.

[25] B. Butschke, M. Schlangen, D. Schröder, H. Schwarz, *Chem. Eur. J.* **2008**, *14*, 11050-11060.

[26] D. Figgen, G. Rauhut, M. Dolg, H. Stoll, *Chem. Phys.* **2005**, *311*, 227-244.

[27] K. A. Peterson, C. Puzzarini, *Theor. Chem. Acc.* **2005**, *114*, 283-296.

[28] L. M. Pratt, S. Voit, B. K. Mai, B. H. Nguyen, *J. Phys. Chem. A* **2010**, *114*, 5005-5015.

[29] D. Vanderbilt, *Phys. Rev. B* **1990**, *41*, 7892-7895.

To be cited as: Chem. Eur. J., 17: 10864–10870. doi: 10.1002/chem.201101551
Version of record: http://dx.doi.org/10.1002/chem.201101551

Figure Legends

Figure 1. Panel **a)**: Positive ion ESI/MS^2 spectrum of $[Cu(hfa)(TMEDA)]^+$ (*m/z* = 386.04842) and schemes for $[Cu(hfa)(TMEDA)]^+$ and for the ionic species at *m/z* = 178.05250 and 115.12287. Panel **b)**: Positive ion ESI/MS^3 spectrum of the ion at *m/z* = 178.05250, and schemes for the ionic species at *m/z* 163.02911 and 150.02125. The parent $[Cu(hfa)_2(TMEDA)]$ scheme is also shown. hfa: CF_3-CO-CH-CO-CF_3^-; TMEDA: $(CH_3)_2N$-CH_2-CH_2-$N(CH_3)_2$; TMEDA(-H): $(CH_3)_2N$-CH_2-CH_2-$N(CH_3)(CH_2)^{\bullet}$. Panel **c):** ball-and-stick representations of the parent $[Cu(hfa)_2(TMEDA)]$ optimized complex, and of the minimum energy structures of the ionic fragments with the corresponding *m/z* values. Color codes: Cu: yellow; C: gray, H: white; N: blue; O: red; F: green.

Figure 2. The $[Cu^{II}(hfa)(TMEDA)]^+$ (initial state) to $(Hhfa)[Cu^{I}(TMEDA(-H))]^{+\bullet}$ (final state) reaction pathway. Red curve: free energy *vs*. reaction coordinate (Q) profile of the exploratory reaction pathway (see movie). Ball-and-stick models: Graphical representations of the optimized geometries for the initial, transition and final states. The calculated values of the barrier [ΔE_{TS} = *E*(transition state) - *E*(initial state)] and the reaction energy [ΔE_r = *E*(final state) - *E*(initial state)] are also reported (in kcal/mol). Upper part of the figure: three occupied molecular orbitals for the optimized transition state geometry, evidencing the participation of the metal d states in the coupled C-H bond homolytic cleavage/interligand proton transfer process. It is shown that the copper(II) center assists the hydrogen abstraction from TMEDA with formation of a *α*-amino radical (center) and the proton delivery to the electron-rich ligand hfa (left), with a single-electron gain (right). A scheme of the copper(II) reduction mechanism (hydrogen abstraction-proton delivery-electron gain) is also reported. Atom color codes: Cu: yellow; C: gray, H: white; N: blue; O: red; F: green.

Figure 3. Evolution of the HOMO (bottom) and LUMO (top) molecular β-spin orbitals from the initial (left) to the final state (right). Initial state: the β-HOMO is localized on the hfa ligand homo, the β-LUMO is predominantly Cu d_{x2-y2}; Cu is in a d^9 configuration [copper(II)]. Transition state: the β-HOMO shows an appreciable Cu d_{x2-y2} contribution and Cu-C* bonding character, while the β-LUMO shows both Cu d_{x2-y2} and (C*N*)-π* character. Here, the Cu d_{x2-y2} state is approximately half-filled ($d^{9.5}$). Final state: the β-HOMO is localized on the $[Cu^{I}(TMEDA(-H))]^{+\bullet}$ six-membered ring, mainly on Cu d_{x2-y2} and N*, while the β-LUMO, localized mainly on the Hhfa ligand lumo, shows no contribution from the copper d-states. The Cu d_{x2-y2} orbital is now fully occupied and copper is in a d^{10} configuration [copper(I)]. The binding energy of $[Cu^{I}(TMEDA(-H))]^{+\bullet}$ with the *β*-diketone enol Hhfa is 23.1 kcal/mol. Atom color codes as in Figure 2.

Figure 4. Spin density distributions (blue isosurfaces) and Mulliken atomic spin densities for: **a)** initial state, $[Cu^{II}(hfa)(TMEDA)]^+$; **b)** transition state; **c)** final state, $(Hhfa)[Cu^{I}(TMEDA(-H))]^{+\bullet}$; **d)** $[Cu^{I}(TMEDA(-H))]^{+\bullet}$. Atom color codes as in Figure 1.

Figure 5. Representations of the geometry and electronic structure of $[Cu(TMEDA(-H))]^{+\bullet}$. a) The six-membered ring 'armchair' structure; b) the α-HOMO, mainly Cu 4s and (C*N*)-π*; c) the α-(HOMO-5), with Cu-d, (C*N*)-π contributions and Cu-C* bonding character; d) the β-HOMO, mainly Cu-d, N-2p and (C*N*)-π; bond lenghts (in Å) for the six-membered ring are also reported. Atom color codes as in Figure 2.

To be cited as: Chem. Eur. J., 17: 10864–10870. doi: 10.1002/chem.201101551
Version of record: http://dx.doi.org/10.1002/chem.201101551

Text for the Table of Contents

New light on Cu chemistry: A Cu^{II}-promoted "hydrogen abstraction-proton delivery-electron gain" mechanism leads to Cu reduction and formation of a Cu^{I}-CNCCN six-member ring showing a novel bonding scheme. Such a single-molecule copper "reduction without reductants" is studied via the fragmentation of a Cu^{II} precursor by combined Electrospray Ionization Mass Spectrometry with multiple collisions experiments and theoretical calculations.

Keywords: copper • density functional calculations • fragmentation reaction • MS • reaction mechanism